Corrosion Behavior of Hydrophobic Coatings in Aqueous CO_2 Environments

Zineb Belarbi
National Energy Technology Laboratory
1450 Queen Avenue SW
Albany, OR 97321
USA
NETL Support Contractor
1450 Queen Avenue SW
Albany, OR 97321
USA

Fangming Xiang
National Energy Technology Laboratory
3610 Collins Ferry Road,
Morgantown, WV 26505
USA
NETL Support Contractor
3610 Collins Ferry Road,
Morgantown, WV 26505
USA

David Hopkinson
National Energy Technology Laboratory
3610 Collins Ferry Road,
Morgantown, WV 26505
USA

Ömer Doğan
National Energy Technology Laboratory
1450 Queen Avenue SW
Albany, OR 97321
USA

ABSTRACT

Steel pipelines, the backbone of natural gas transportation, face a significant challenge: internal corrosion. Internal corrosion is caused by gas impurities such as CO_2, moisture, and H_2S, leading to material degradation. To combat this, the National Energy Technology Laboratory (NETL) developed a novel hydrophobic coating to reduce surface hydrophobicity and enhance the corrosion resistance of steel. NETL's approach uses multi-layer hydrophobic coatings, a novel and promising coating that could potentially revolutionize the industry's approach to internal corrosion mitigation. This work aims to investigate the corrosion performance of the hydrophobic coating and determine the water uptake. Electrochemical corrosion experiments were carried out on bare X65 carbon steel without and with coating in 3.5 wt.% NaCl saturated with CO_2 at 20 °C to follow the water uptake as a function of exposure time. Linear polarization resistance (LPR) was used to determine the corrosion rate for carbon steel immersed in a NaCl electrolyte saturated with CO_2. Electrochemical impedance spectroscopy (EIS) of uncoated and coated bare carbon steel was investigated. The analyses of impedance models and water uptake behaviors of hydrophobic coatings were studied for 200 hours during the corrosion process. The water uptake was estimated using the Brasher and Kingsbury relation. The corrosion of the base metal without coating (3.8 mm/y) was compared to coated carbon steel (0.02 mm/y). The results showed that the superhydrophobic coating that was developed used innovative nano-based materials to act as protection layers on the surface of metallic parts against mechanical aggressors, corrosion, and fouling agents. These coatings have proven to be ideal candidates to protect steel pipelines.

Keywords: CO_2 corrosion, natural gas pipelines, coatings, hydrophobicity, Carbon steel.

INTRODUCTION

Natural gas pipelines are subject to internal corrosion, which is enhanced by moisture and impurities such as carbon dioxide (CO_2), hydrogen sulfide (H_2S), and oxygen (O_2). The National Association of Corrosion Engineers (NACE) performed a cost study and found that the yearly corrosion costs in the oil and gas industry are estimated to be approximately $1.372 billion[1,2]. In addition to the economic costs, internal corrosion can lead to structural failures of steel pipelines, which may cause dramatic consequences for humans and the surrounding environment. According to a National Energy Technology Laboratory (NETL) survey, 112 (12%) incidents reported in U.S. natural gas transmission lines were due to internal corrosion[3,4]. Proper design, operation, and prevention could avoid the yearly corrosion costs. Several prevention methods have been suggested to mitigate internal corrosion, such as corrosion inhibitors and internal coatings. Injection of corrosion inhibitors into gas streams in natural gas transmission lines is challenging because of the non-homogeneous distribution of the inhibitors to all areas of the pipe[5-8]. Therefore, internal coatings are one of the most widely used solutions to reduce internal corrosion. Adding a protective coating to the inner pipe surface can reduce corrosion, but conventional polymer coatings (e.g., epoxy, polyethylene, polyurethane, etc.) are insufficient for long-term corrosion resistance[9,10]. These coatings allow corrosive species to permeate and accumulate on the steel-coating interface. This will cause corrosion underneath the coating (i.e., under film corrosion), eventually developing into surface blisters and localized pitting corrosion[11].

To enhance the long-term corrosion resistance of the internal coatings, several studies were performed on reducing the permeability of the coating and reducing the contact area with corrosive species. Many studies showed that adding graphene, clay, and Mxene nanosheets into a polymer matrix could help reduce the permeability of the resultant composite coating by extending the permeation path for small molecules, ultimately leading to lower corrosion rates. Chang et al.[12] found that adding 0.5 wt.% functionalized graphene into polyaniline can increase the protection efficiency to 53.49%. Chiong et al.[13] claimed that adding 0.4 wt.% graphene oxide to polyvinylidene fluoride effectively improves the corrosion resistance of carbon steel in salt spray and acid immersion tests. Andsaler et al.[14] added multilayer graphene into epoxy, reducing the corrosion rate by three times. However, there are a few challenges with nanosheets, especially graphene: (1) the nanosheets can be too expensive to be used on a large scale. (2) None of the studies managed to align the nanosheets within the polymer matrix, which prevents the barrier capabilities of nanosheets from being fully realized. To overcome these challenges, superhydrophobic materials can be used to reduce the permeability of the coating and reduce the contact area with corrosive species. Xiang et al.[15] prepared a bimetallic Ni/Cr_2O coating with a water contact angle of 167.9 and achieved a corrosion current density of 2.52×10^{-8} A/cm^2. Ye et al.[16] developed a superhydrophobic coating based on oligoaniline-modified silica nanoparticles, which improved corrosion resistance in a 3.5 wt.% NaCl solution. Ma et al.[17] created a biomimetic liquid-infused slipper surface on carbon steel and observed improved anti-corrosion performance due to its anti-wetting capability. Despite the progress made in developing a superhydrophobic coating for carbon steel, there is still plenty of room for improvement. More superhydrophobic coatings have been designed to protect steel from marine corrosion[18]. These coatings lessen the reaction between aqueous corrosive species and steel substrates and reduce the water-solid contact area in the marine environment[19].To the best of our knowledge, there is no field study of a superhydrophobic internal coating that can extend the service life of natural gas pipelines.

NETL developed a novel hydrophobic coating to mitigate internal corrosion, reduce surface hydrophobicity, and enhance steel's corrosion resistance. NETL's approach uses multi-layer hydrophobic coatings, a novel and promising coating that could potentially revolutionize the industry's approach to internal corrosion mitigation. This work aims to investigate the corrosion performance of the hydrophobic coating and determine the water uptake. Superhydrophobic coatings are based on hydrophobic materials with microscopic surface roughness, which can trap air on the surface and thus increase the effective contact angle.

EXPERIMENTAL PROCEDURE

MATERIALS AND CHEMICALS

Positively charged polymers (known as polycations) and negatively charged silica nanoparticles (known as polyanions) were purchased from Sigma Aldrich and used as received. All components were dissolved in methanol or water to prepare 0.1 wt.% dipping solutions. Specimens made of API 5L X65 pipe grade (0.075 in. thick, Nippon) were machined into rectangular pieces within 3.5 x 2.5 inches as substrates.

LAYER-BY-LAYER DEPOSITION

A layer-by-layer assembly technique was used to deposit multilayers on carbon steel substrates to form superhydrophobic coatings. Before the deposition process, the steel substrates were polished using 400 and 600-grit sandpaper and then rinsed in acetone. A custom-built robotic dipping system, which was similar to the device reported by Jang and Grunlan[20] was used to prepare superhydrophobic coatings. The carbon steel substrate was dipped in a 0.1 wt.% polycation solution for 5 minutes (Figure 1, Step 1) and then rinsed with methanol for 10 seconds, three times, to eliminate loosely deposited polycations on the steel surface (Figure 1, Step 2). This procedure allowed a layer of polycation molecules to adsorb on the substrate through coordinate and/or ionic bonding. After that, carbon steel coated with the polycation layer was dipped in a 0.1 wt.% polyanions solution for 5 minutes (Figure 1, Step 3) and rinsed with water for 10 seconds, three times, to eliminate access or loosely deposited polyanions on the coated carbon steel surface (Figure 1, Step 4). The combination of one polycations layer and one polyanions layer is known as one bilayer. The surface charge of the substrate would be reversed after each deposition, allowing oppositely charged components to deposit alternately. After this initial bilayer was deposited, additional bilayers were added using similar dipping and rinsing procedures (Figure 1). One minute of dipping was used. This procedure was repeated until a set number of bilayers were deposited. Once the layer-by-layer assembly was completed, the coating was transformed from hydrophilic to superhydrophobic by reacting with hydrophobic silane via chemical vapor deposition.

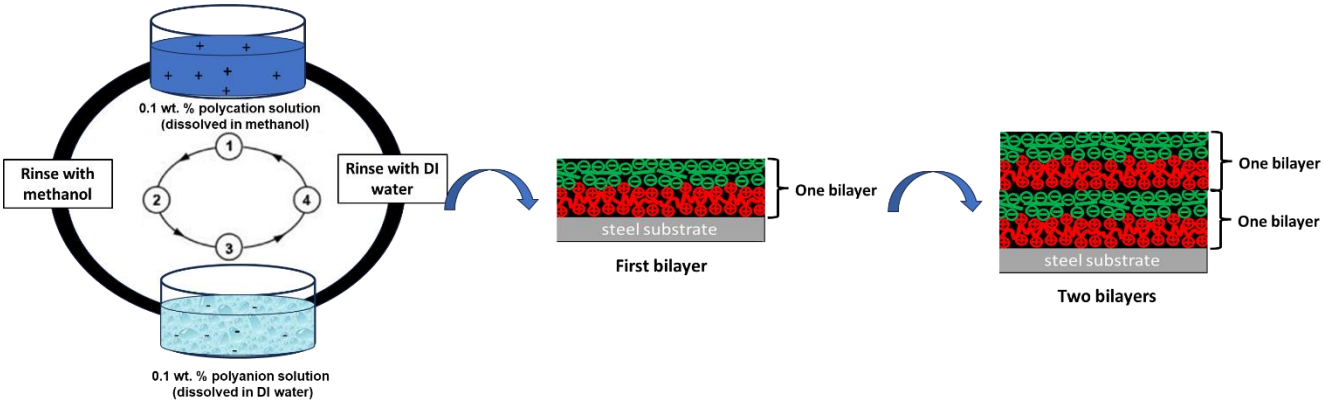

Figure 1: Illustration of different steps for a layer-by-layer assembly technique.

ELECTROCHEMICAL MEASUREMENTS

A three-electrode flat glass cell setup (Figure 2), similar to one used in previous studies[21], was used to perform conventional electrochemical measurements on uncoated and coated carbon steel in 3.5 wt.% NaCl saturated with CO_2 at 20 °C. Uncoated and coated steel specimens with an exposed surface area of 1 cm^2 were used as the working electrode. A saturated calomel reference electrode (SCE) was connected externally to the cell via a Luggin capillary with a porous glass tip. The counter electrode was made of a platinum mesh. Before the insertion of the specimens and to eliminate the dissolved oxygen in the solution, the solution was purged with CO_2 gas for 2 to 3 hours to reach an equilibrium pH of 3.8 to 3.9. All the corrosion tests were conducted at ambient temperature (20 °C ±0.1). Uncoated carbon steel was used as a baseline. Before the test, the uncoated carbon steel specimen was ground using silicon carbide paper (400 and 600 grit), rinsed with isopropanol in an ultrasonic cleaner for 2 to 3 minutes,

and air-dried. To maintain the saturation level of CO_2 in the solution and avoid oxygen ingress, the solution was continuously sparged with CO_2 during the entire test. The open-circuit potential (OCP) was recorded for 60 minutes to ensure a stable signal before all the electrochemical measurements. Potentiodynamic polarization (PDP) measurements were recorded from -0.33 V vs. OCP to +0.66 V vs. OCP at a scan rate of 1 mV/s. The Tafel values (β_a and β_c) for these experiments were determined by Tafel's extrapolation method applied to PDP curves. The corrosion behavior of uncoated and coated carbon steel was monitored every hour during a total exposure time of 24 hours by measuring the resistance of polarization R_p using linear polarization resistance (LPR) and electrochemical impedance spectroscopy (EIS). The polarization resistance of R_p was measured using LPR by polarizing the working electrode from -5 mV to +5 mV vs. OCP, using a scan rate of 0.125 mV/s. A long-term corrosion test was performed to investigate the corrosion performance of the superhydrophobic coating. The corrosion current I_{corr} was calculated considering the Stern-Geary assumption (Equation 1)[22].

$$I_{corr} = \frac{1}{R_p} * \frac{\beta_a * \beta_c}{2.303 * (\beta_a + \beta_c)} \quad (1)$$

The corrosion rate was calculated using the following Equation[22]:

$$CR = K * \frac{I_{corr} * EW}{\rho * A} \quad (2)$$

Where *CR* is corrosion rate in mm/y; *K*: conversion factor (3,270 mm.g/A.cm. y); EW: equivalent weight (27.92 g/equivalent); *A*: area in cm^2; ρ: density of substrate (7.87 g/cm^3) I_{corr}: corrosion current in A. EIS measurements were carried out over 100 kHz to 10 mHz using an AC amplitude of 10 mV (RMS) to identify water uptake by superhydrophobic coating. The water uptake is the amount of water/solution in the superhydrophobic coating, which is essential to assessing the anticorrosive protection of the coating. The most used model for estimating water uptake by a film is based on Brasher and Kingsbury's Equation[23]:

$$\phi_{water} = \frac{\log\left(C_{film}/C_0\right)}{log\varepsilon_{water})} \quad (3)$$

Where C_{film}: capacitance of the film with time; C_0: capacitance of the film coating at t=0; ε_{water}: dielectric constant of water = 80, Φ_{water}: water content: a volume fraction of water at the time t. Electrochemical measurements were carried out using a Gamry Reference 600+[¥] potentiostat/galvanostat. To verify the reproducibility of the results, all the electrochemical tests were repeated two to three times. The test matrix is shown in Table 1.

[¥]Trade name

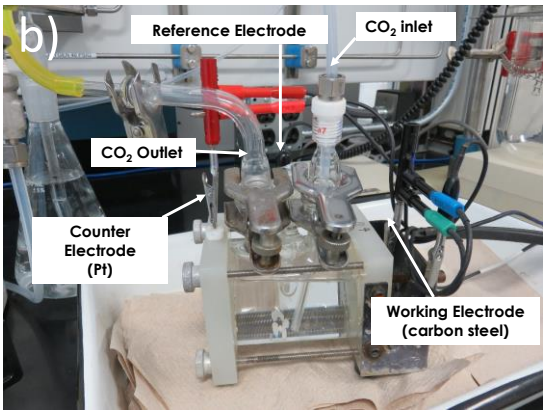

Figure 2: Flat electrochemical cell with three electrodes configuration.

Table 1: Experimental Matrix for Electrochemical Tests

Total pressure (bar)	1
pCO_2 (bar)	0.97
Solution temperature (°C)	20 ± 0.1
Solution	0.25 L of 3.5 wt.% NaCl
pH	3.88
Tested steels	X65 carbon steel Coated X65 carbon steel
Duration (days)	8

RESULTS

CORROSION TESTS: POTENTIODYNAMIC POLARIZATION CURVE

Figure 3 shows a PDP diagram for uncoated and coated carbon steel in 3.5 wt.% NaCl saturated with CO_2 at ambient temperature (20 °C). As shown in Figure 3, uncoated steel shows a typical anodic polarization behavior above the OCP of carbon steel in NaCl solution, consisting of active dissolution (iron dissolution, Equation 4), passivity, and a rapid increase in the current density due to pitting. Below the OCP is the cathodic region where the hydrogen evolution via the reduction of H^+ (Equation 5) and water molecule) are taking place. The source of H^+ comes from the dissociation of carbonic acid, which was formed from dissolved CO_2 in water (Equations 6 to 8). Iron ions react with carbonate ions to form a corrosion product if saturation is reached (Equation 9).

$$Fe \overset{1}{\Leftrightarrow} Fe^{2+} + 2\,e^- \quad (4)$$

$$2\,H^+ + 2\,e^- \overset{1}{\Leftrightarrow} H_2 \quad (5)$$

$$CO_2 + H_2O \overset{1}{\Leftrightarrow} H_2CO_3 \quad (6)$$

$$H_2CO_3 \overset{1}{\Leftrightarrow} HCO_3^- + H^+ \quad (7)$$

$$HCO_3^- \overset{1}{\Leftrightarrow} CO_3^{2-} + H^+ \quad (8)$$

$$CO_3^{2-} + Fe^{2+} \overset{1}{\Leftrightarrow} FeCO_3 \quad (9)$$

The superhydrophobic coating shifted the corrosion potential to a more anodic potential, decreasing the current density (Table 2), which reduced the corrosion rate. The superhydrophobic coating formed a physical barrier for water and corrosive species to diffuse towards the metal surface[18,19]. The corrosion kinetic parameters E_{corr}, i_{corr}, and CR for uncoated and coated carbon steel with Zn cold spray coatings are shown in Table 2.

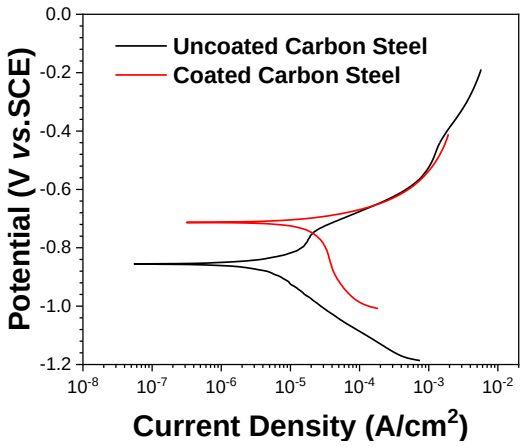

Figure 3: PDP curves of uncoated and coated steel with ZnNb in conditions with and without flow. This graph shows Potential (V vs. SCE) vs. Current Density (A/cm^2).

Table 2: Corrosion Kinetic Parameters E_{corr}, i_{corr}, and CR for Uncoated and Coated Carbon Steel Immersed in a 3.5 wt.% NaCl Solution Saturated with CO_2 at 20 °C

Alloys	E_{corr} (V vs. SCE)	i_{corr} (A/cm^2)	β_a (V/decade)	β_c (V/decade)	CR (mm/y)
Uncoated carbon steel	-0.85	5.35 x 10^{-5}	0.530	0.496	0.62
Coated carbon steel	-0.71	1.3 x 10^{-5}	0.462	0.975	0.15

LINEAR POLARIZATION RESISTANCE

The OCP was monitored for 1 hour pre-corrosion before the first LPR curves were recorded. Figure 4 shows the variation of corrosion rate and OCP of uncoated and coated carbon steel immersed in 3.5 wt.% NaCl saturated with CO_2 over time. The average corrosion rate (Figure 4a) for uncoated and coated carbon steel is approximately 3.8 mm/y and 0.02 mm/y, respectively. Figure 4b shows that the steady-state potential for uncoated carbon steel is -0. 75 V. However, the initial potential for coated carbon steel was -0.60 V and then dropped to a negative value of -0.68 V after 24 hours of exposure. This effect was due to superhydrophobic coating, which lessens the reaction between aqueous corrosive species and carbon steel substrate and reduces the water-solid contact area. Coated carbon steel's average corrosion rate increased to a steady state value of 0.1 mm/y after 100 hours of exposure (Figure 5a). The OCP continued to shift to a more negative value until it reached a steady-state value of -0.71 V after 100 hours of exposure (Figure 5b). The increase in corrosion rate is due to diffusion of the water through the superhydrophobic coating, which causes the active dissolution of iron (Equation 4), which increases the pH (accelerates the cathodic reaction, Equation 5) at the interface surface/electrolyte. Once the water uptake by the coating reached a saturated value, the corrosion rate stabilized.

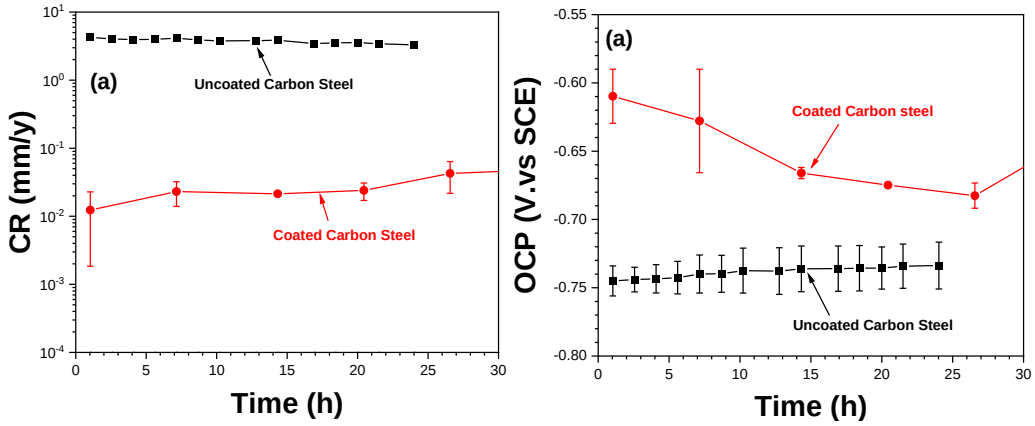

Figure 4: Average corrosion rate (a) and open circuit potential (b) of uncoated and coated carbon steel immersed in 3.5 wt.% NaCl solution saturated with CO_2 at 20 °C as a function of time.

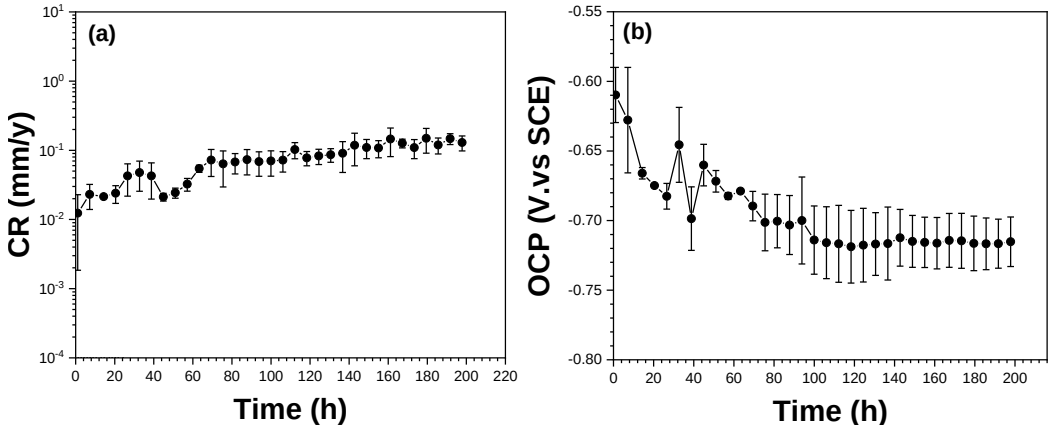

Figure 5: Average corrosion rate (a) and open circuit potential (b) of coated carbon steel immersed in 3.5 wt.% NaCl solution saturated with CO_2 at 20 °C as a function of time.

ELECTROCHEMICAL IMPEDANCE SPECTROSCOPY

EIS measurements were performed to complement the LPR results. Figure 6 shows the Nyquist plots and Bode diagram of uncoated carbon steel as a function of immersion time in 3.5 wt.% NaCl solution saturated CO_2. The Nyquist diagram (Figure 6a) exhibits one high-frequency capacitive and low-frequency inductive loop. The high-frequency semicircle is associated with the time constant of the charge transfer process and the double-layer capacitance (C_{dl}). The inductive loop may be attributed to the relaxation process obtained by adsorbed species such as Cl^- and H^+ on the electrode surface. The EIS diagram (Figure 6) showed similar characteristics to the known corrosion behavior of bare steel in the CO_2 environment[4-6,21]. The low-frequency limit of the impedance (Figure 6a and 6b) increased with time; this could be due to the corrosion product layer formed on the steel surface, which slowed down the dissolution of iron. Figure 7 presents the impedance diagrams plotted at OCP for coated carbon steel after immersion in a 3.5 wt.% NaCl solution saturated with CO_2. The low-frequency limit of the impedance loop increased for coated carbon steel (Figure 7a, Figure 7b) compared to uncoated carbon steel (Figure 6), indicating an increase in polarization resistance and a decrease in corrosion rate, as shown in Figure 4. This result confirms that the superhydrophobic coating is effective in a CO_2-aqueous environment. In addition, the impedance modulus value of coated carbon steel was 200 times higher than that of uncoated steel (Figure 7c), and a shift and decrease in the phase (Figure 7c) were also observed. The low-frequency response differs from uncoated carbon steel. In addition to the time constant of the charge transfer process (R_t) and double layer capacitance (C_{dl}), a second-time constant was observed in the low-frequency domain, which can be attributed to the corrosive species diffusing through the superhydrophobic coating. Figure 8 presents the Nyquist diagrams and bode plots of coated carbon steel obtained in a 3.5 wt.% NaCl solution after different immersion times. The low-frequency limit of the

impedance decreased (Figure 8a, Figure 8b) after two days of exposure, and insignificant changes in the impedance were observed after seven days of exposure. An increase and no shift in the phase diagram (Figure 8 c) were observed after two days of exposure to a corrosive environment.

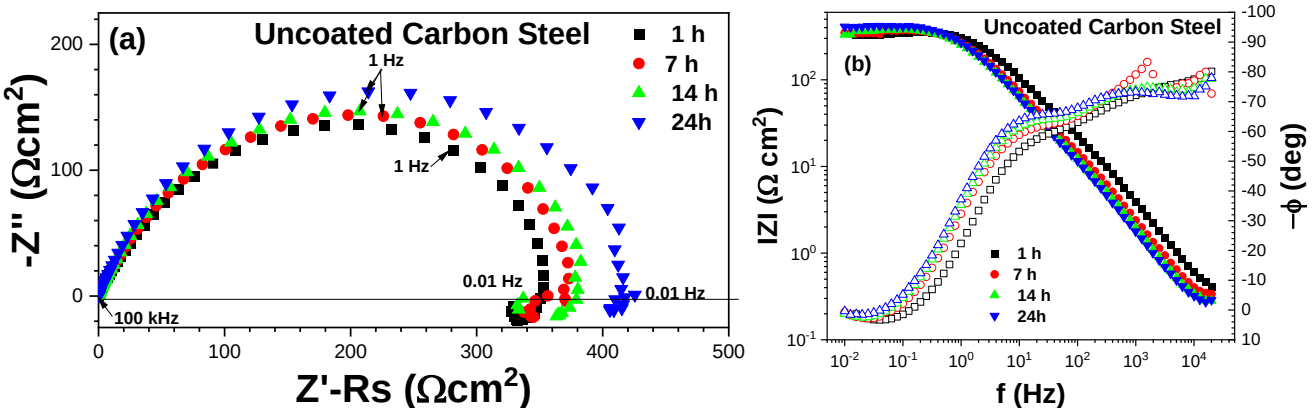

Figure 6: Nyquist diagrams (a) and Bode diagrams (b) (modulus (■ ● ▲), phase angle (□ ○ Δ) of uncoated carbon steel immersed for 24 hours in a 3.5 wt.% NaCl solution saturated with CO_2 at 20 °C.

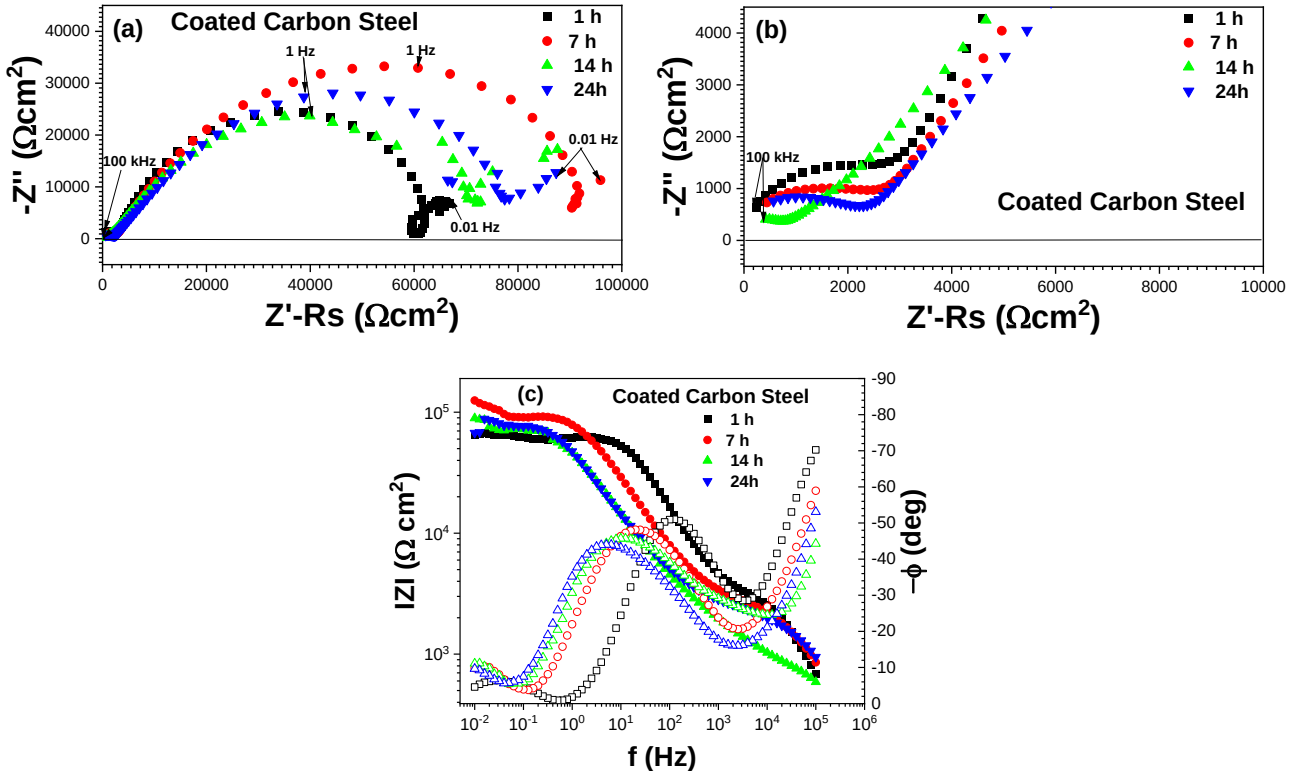

Figure 7: Nyquist diagrams (a, b) and Bode diagrams (c) (modulus (■ ● ▲), phase angle (□ ○ Δ) of coated carbon steel immersed for 24 hours in a 3.5 wt.% NaCl solution saturated with CO_2 at 20 °C.

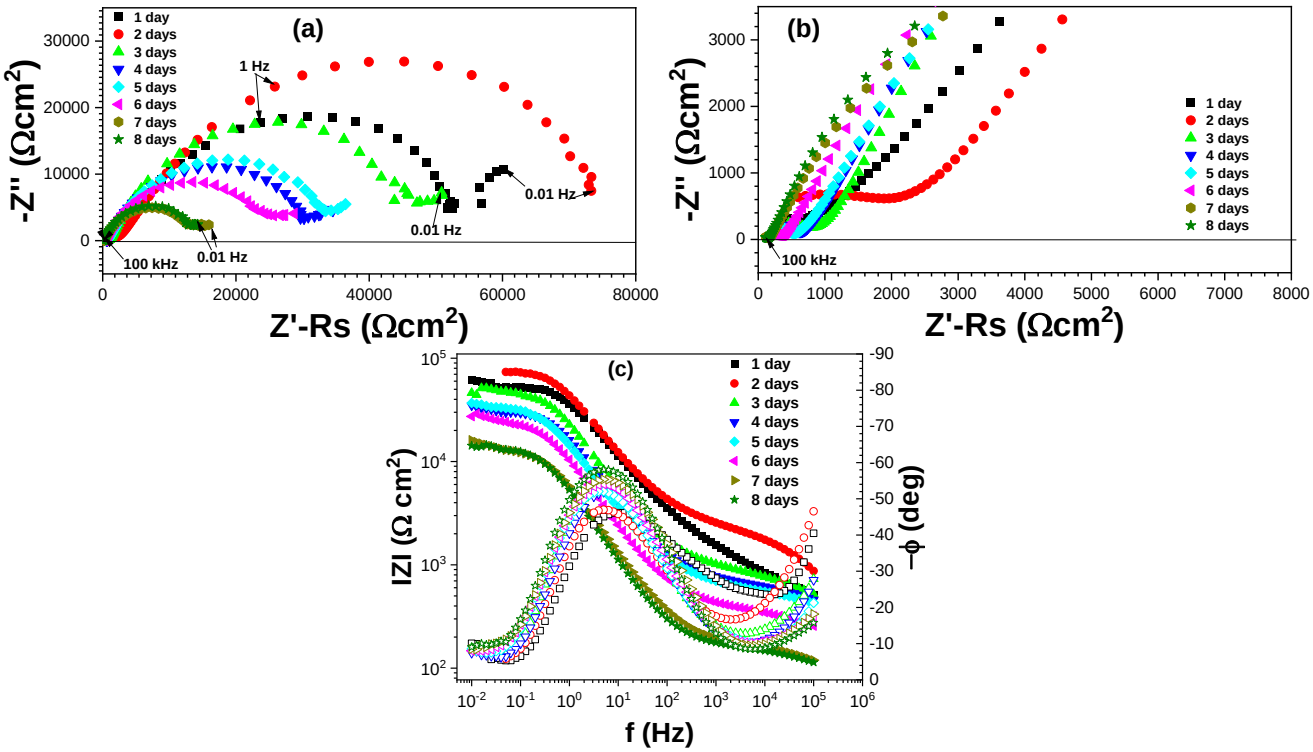

Figure 8: Nyquist diagrams (a, b) and Bode diagrams (c) (modulus (■ ● ▲), phase angle (□ ○ Δ) of coated carbon steel immersed in a 3.5 wt.% NaCl solution saturated with CO_2 at 20 °C, after 24 hours.

Figure 9 shows the electrical equivalent circuit used to fit the EIS experimental data in Figure 7 and Figure 8. To calculate the double-layer capacitance (C_{dl}) and film capacitance of the superhydrophobic coating (C_{film}), Brug's formula[24] (Equation 10) and HHu and Mansfeld's formula[25] (Equation 11) were used, respectively. Where R_t is the charge transfer resistance, R_{film} is the film resistance, R_s is the electrolyte resistance, Q_{dl} and α are double-layer CPE_{dl} coefficients. Q_{film} and α_f are film capacitance (CPE_{film}) coefficients.

$$C_{dl} = Q_{dl}^{\frac{1}{\alpha}} * \left(\frac{R_s * R_t}{R_s + R_t}\right)^{\frac{(1-\alpha)}{\alpha}} \qquad (10)$$

$$C_{film} = Q_{film}^{\frac{1}{\alpha f}} * \left(R_{film}^{\frac{(1-\alpha f)}{\alpha f}}\right) \qquad (11)$$

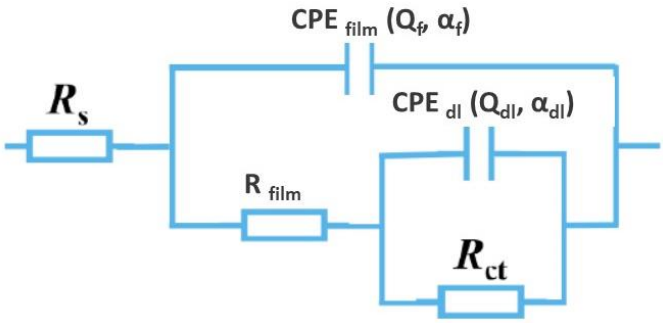

Figure 9: Equivalent circuit used for the regression calculation of experimental data presented in Figure 7 and Figure 8.

The estimated value of solution resistance R_s in all cases was approximately 28 Ω·cm^2. The values of R_t measured with EIS were used to calculate the corrosion rate using Equations (1) and (2). The results are shown in Figure 10. The corrosion rates measured using EIS are comparable to those measured by LPR, confirming the corrosion resistance of the superhydrophobic coating. Figure 11 shows the variation of C_{dl}, R_{film}, C_{film}, and water uptake (ϕ) with immersion time. Figure 11a presents the evolution of C_{dl} with time. After one hour of immersion, the value of C_{dl} was between 0.02 µF/cm^2 and 0.09 µF/cm^2. After 48 hours (two days) of immersion, the C_{dl} increased to 4.5 µF/cm^2. The C_{dl} of bare or uncoated carbon steel usually is between 10 µF/cm^2 and 50 µF/cm^2 [4-6]. The C_{dl} measured on coated carbon steel was smaller than those on uncoated carbon steel; this could be due to superhydrophobic coating which reduces the diffusion of corrosion species and water to the steel surface and protects the metal from corrosion. The extracted value for the film capacitance (Figure 11b) increased from 0.0028 to 0.005 µF/cm^2 due to the superhydrophobic coating's physical and electrical properties (Figure 11c), which is dependent on the water uptake (ϕ) by the coating. Figure 11d depicts values estimated for the water uptake of the superhydrophobic coating using Brasher and Kingsbury's equation (Equation 3). Before exposure to the electrolyte, the superhydrophobic coating is dry; the water uptake is 0%. After 1 hour of exposure to the electrolyte, the water uptake increased to 8%. After 48 hours, the water uptake reached a stable value of 20%. This could be due to diffusion of water and corrosive species through the coatings, which cause an increase in corrosion rates (Figure 10). Overall, the low water uptake of the superhydrophobic coating demonstrated its corrosion resistance. As the literature describes, other multiple empirical models can be used to estimate the water uptake of organic coatings. However, estimated water uptake using the Brasher and Kingsbury model (Equation 3) better agrees with gravimetry than other empirical models[19,26,27]. Nguyen et al.[28] found that the estimated water uptake by the Brasher and Kingsbury formula yielded water uptake values much higher than those measured directly by gravimetry.

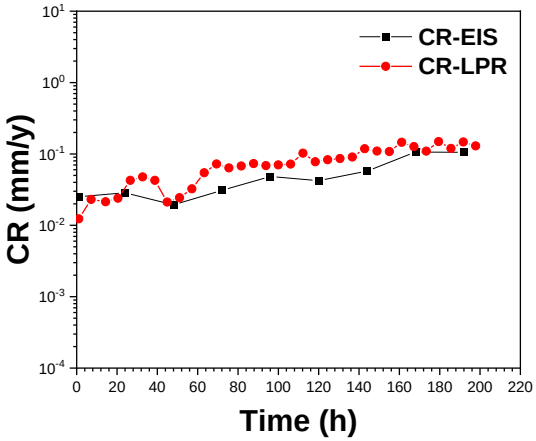

Figure 10: LPR and EIS average corrosion rate of coated carbon steel immersed in 3.5 wt.% NaCl solution saturated with CO_2 at 20 °C as a function of time.

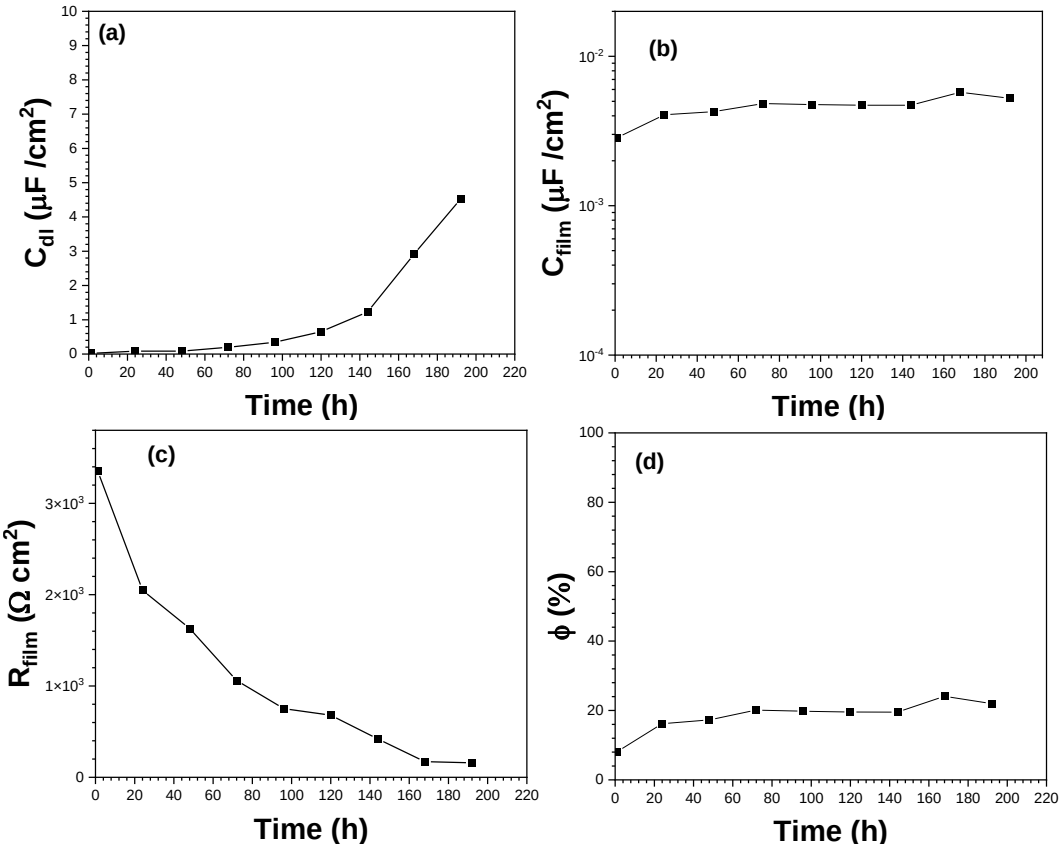

Figure 11: C_{dl} (a), C_{film} (b), $R_{film,}$ (c), and ϕ (d) of coated carbon steel immersed in 3.5 wt.% NaCl solution saturated with CO_2 at 20 °C as a function of time.

CONCLUSIONS

The corrosion performance of the hydrophobic coating was investigated in 3.5 wt.% NaCl saturated with CO_2 at 20 °C. The water uptake was estimated using the Brasher and Kingsbury relation. The corrosion of the base metal without coating (3.8 mm/y) was compared to coated carbon steel (0.02 mm/y). The superhydrophobic coating exhibited good behavior against CO_2 corrosion. The low water uptake of the superhydrophobic coating demonstrated its corrosion resistance. The results showed that the superhydrophobic coating was developed using innovative nano-based materials to act as protection layers on the surface of metallic parts against mechanical aggressors, corrosion, and fouling agents. These coatings have proven to be ideal candidates to protect steel pipelines.

DISCLAIMER

This project was funded by the United States Department of Energy, National Energy Technology Laboratory, in part, through a site support contract. Neither the United States Government nor any agency thereof, nor any of their employees, nor the support contractor, nor any of their employees, makes any warranty, express or implied, or assumes any legal liability or responsibility for the accuracy, completeness, or usefulness of any information, apparatus, product, or process disclosed, or represents that its use would not infringe privately owned rights. Reference herein to any specific commercial product, process, or service by trade name, trademark, manufacturer, or otherwise does not necessarily constitute or imply its endorsement, recommendation, or favoring by the United States Government or any agency thereof. The views and opinions of authors expressed herein do not necessarily state or reflect those of the United States Government or any agency thereof.

ACKNOWLEDGEMENTS

This work was performed in support of the U.S. Department of Energy's (DOE) Office of Fossil Energy and Carbon Management's Emissions Mitigation Research Program and executed through the National Energy Technology Laboratory (NETL) Research & Innovation Center's Natural Gas Infrastructure Field Work Proposal. The authors of this project report would like to thank the technician, Trevor Godell, for machining the samples.

REFERENCES

1. G. H. Koch, M. P. H. Brongers, N. G. Thompson, Y. P. Virmani, J. H. Payer, Corrosion Cost and Preventive Strategies in the United States, CC Technologies, Inc.; NACE International; United States. Federal Highway Administration. Office of Infrastructure Research and Development, FHWA-RD-01-156, R315-01 2002-03-01,
2. A. Khattak, Corrosion in the oil and gas industry: A costly challenge, Oil and Gas News 41, 9 (2024).
3. D. Justman, K. Rose, J. Bauer, NETL, 2017. Data analyzed from U.S. DOT PHMSA incident data.
4. Z. Belarbi; Richard. E. Chinn; Ö. N. Doğan, "Corrosion of zinc cold spray coatings in a wet sweet and sour gas environment," Corrosion 80,7 (2024): p.676.
5. Z. Belarbi, F. Farelas, M. Singer, S. Nesic, "Role of amines in the mitigation of CO_2 top-of-the-line corrosion", Corrosion 72,10 (2016): p. 1300.
6. Z. Belarbi, J.M. Dominguez Olivo, F. Farelas, M. Singer, D. Young, S Nesic, "Decanethiol as a corrosion inhibitor for carbon steels exposed to aqueous CO_2", Corrosion 75, 10 (2019): p. 246.
7. Z. Belarbi, F. Farelas, D. Young, M. Singer, S Nesic, "Effect of operating parameters on the inhibition efficacy of decanethiol", CORROSION/2018, paper no 10823 (Houston, TX: NACE, 2018).
8. Y. He, S. Ren, X. Wang, D. Young, M. Singer, Z. Belarbi, M. Mohamed-Saïd, S. Camperos, Md R. Khan, K. Cimatu, "Delinkage of metal surface saturation concentration and micellization in corrosion inhibition", Corrosion 78, 7(2022): p. 625.
9. M. Matthew Ali, C. J. Magee, P. Y. Hsieh "Corrosion protection of steel with metal-polymer composite barrier liners," Journal of Natural Gas Science and Engineering 81, 103407 (2020): p. 1.
10. G. Siegmund, G. Schmitt, J. Noga, B. Sadlowsky, " Permeation damage of polymer liner in oil and gas pipelines: A Review" Polymer 12, 10 (2020): P.2307-1.
11. E. Lapushkina," Anti-corrosion coatings fabricated by cold spray technique: Optimization of spray condition and the relationship between microstructure and performance Materials," Université de Lyon; Tohoku Gakuin University (Sendai, Japon), 2020.
12. C. H. Chang, T. C. Huang, C. W. Peng, L. C. Yeh, H. I. Lu, W. I. Hung, C. J. Weng, J. M. Yang, "Novel anticorrosion coatings prepared from polyaniline/graphene composites," Carbon 50, 14 (2012): p. 5044.
13. S. J. Chiong, P. S. Goh, A. F. Ismail, "Novel hydrophobic PVDF/APTES-GO nanocomposite for natural gas pipelines coating," Journal of Natural Gas Science and Engineering 42, (2017): p. 190.
14. A. R. Andsaler, W. Philip, I. Sudin, M. Z. M. Yusop, "Effects of graphene polymer nanocomposite coating on corrosion resistance of ASTM A106 carbon steel pipe", Malaysian Journal of Fundamental and Applied Sciences 16, 4 (2020): p. 483.
15. T. Xiang, D. Chen, Z. Lv, Z. Yang, L. Yang, C. Li, "Robust superhydrophobic coating with superior corrosion resistance," Journal of Alloys and Compounds 798 (2019): p. 320.

16. Y. Ye, Z. Liu, W. Liu, D. Zhang, H. Zhao, L. Wang, X. Li, “Superhydrophobic oligoaniline-containing electroactive silica coating as pre-process coating for corrosion protection of carbon steel,” Chemical Engineering Journal 348, (2018): p.940.
17. Q. Ma, W. Wang, G. Dong, G., “Facile fabrication of biomimetic liquid-infused slippery surface on carbon steel and its self-cleaning, anti-corrosion, anti-frosting and tribological properties,” Colloids and Surfaces A: Physicochemical and Engineering Aspects 577 (2019): p.17.
18. A. O. Ijaola, P. K. Farayibi , E. Asmatulu, “Superhydrophobic coatings for steel pipeline protection in oil and gas industries: A comprehensive review,” Journal of Natural Gas Science and Engineering 83, (2020):p. 103544.
19. M. Ferrari, A. Benedetti, F. Cirisano, “Superhydrophobic coatings from recyclable materials for protection in a real sea environment,” Coatings 9, 5 (2018): p. 303.
20. W. Jang, J. C. Grunlan, “Robotic dipping system for layer-by-layer assembly of multifunctional thin films,” *Review of Scientific Instruments* 76, 103904 (2005).
21. Z. Belarbi, P. D. Jablonski,O. N. Dogan, M. Detrois, R. P. Oleksak, "Effect of Minor Ce Additions on Corrosion Behavior of Experimental Pipeline Steel." Paper presented at the AMPP Annual Conference + Expo, New Orleans, Louisiana, March 2024, paper no 20450.
22. Z. Belarbi; Richard. E. Chinn; Ö. N. Doğan, “Corrosion of zinc cold spray coatings in a wet sweet and sour gas environment,” Corrosion 80,7 (2024): p.676.
23. D.M. Brasher, A.H. Kingsbury,” Electrical measurements in the study of immersed paint coatings on metal. I. Comparison between capacitance and gravimetric methods of estimating water-uptake”, Journal of Applied Chemistry 4, 2 (1954): p. 62.
24. J. Brug, A.G.V.D. Eeden, M. Sluyters-Rehbach, J.H. Sluyters, "The analysis of electrode impedances complicated by the presence of a constant phase element ", Journal of Electroanalytical Chemistry and interfacial electrochemistry 176, (1984): p. 275.
25. C. H. Hsu; F. Mansfeld, “Technical Note: Concerning the Conversion of the Constant Phase Element Parameter Y_0 into a Capacitance”, Corrosion 57, 9 (2001) p: 747.
26. R.G. Duarte, A.S. Castela, M.G.S. Ferreira, “A new model for estimation of water uptake of an organic coating by EIS: The tortuosity pore model”, Progress in Organic Coatings 65, 2 (2009): p. 197.
27. X. Yuan, Z.F. Yue, X. Chen, S.F. Wen, L. Li, T. Feng, “EIS study of effective capacitance and water uptake behaviors of silicone-epoxy hybrid coatings on mild steel”, Progress in Organic Coatings 86, (2015): p. 41.
28. A. S. Nguyen, N. Causse, M. Musiani, M. E. Orazem, N. Pébèrea, B. Tribollet, V. Vivier, “Determination of water uptake in organic coatings deposited on 2024 aluminum alloy: Comparison between impedance measurements and gravimetry”, Progress in Organic Coatings 112, (2017): p. 93–100.